Multiscale Clustering in Granular Surface Flows

Daniel Bonamy, François Daviaud, Louis Laurent, Marco Bonetti,

Jean-Philippe Bouchaud

Multiscale Clustering in Granular Surface Flows

D. Bonamy, F. Daviaud, L. Laurent, M. Bonetti, and J. P. Bouchaud

Service de Physique de l'Etat Condensé, CEA/DSM Saclay, 91191 Gif sur Yvette, France
(Received 20 September 2001; published 25 June 2002)

We investigate steady granular surface flows in a rotating drum and demonstrate the existence of rigid clusters of grains embedded in the flowing layer. These clusters appear to be fractal and their size is power law distributed from the grain size scale up to the thickness of the flowing layer. The implications of the absence of a characteristic length scale on available theoretical models of dense granular flows are discussed. Finally, we suggest a possible explanation of the difference between velocity profiles observed in surface flows and in flows down a rough inclined plane.

Granular materials share properties with both usual liquids and solids. They can form an inclined free surface without flowing, but when the angle of the free surface exceeds some threshold value, an avalanche occurs. Global behaviors can be described by models derived from fluid mechanics [1,2] or nonlinear physics [3,4]. However, some experimental results remain far from being understood. Detailed measurements of the mean density profile and the mean tangential velocity profile obtained in three-dimensional flow (3D) by NMR [5] and in two-dimensional flows (2D) by direct image analysis [6,7] show strong evidence that the relation between stress and strain is *nonlocal:* (i) the velocity gradient is found to be constant in the flowing layer whereas momentum balance predicts a linear variation of the shear stress with depth [8]; (ii) the velocity gradient presents a different scaling with the depth for dense granular flows down a rough inclined plane [9] indicating the nonlocal influence of boundary conditions on internal rheology inside the flowing layer; (iii) the velocity gradient does not vanish at the free surface at variance with typical fluids. Very recent models have tried to account for some nonlocal effects [6,8,10]. We report here the first experimental evidence of rigid clusters of grains embedded in the flow and characterize their geometrical and statistical properties. Although clustering instabilities driven by the inelasticity of grain collision are well known in granular gases [11], they have never been observed in dense surface flows. We find that these clusters are fractal and their size is power law distributed from the microscopic scale—the diameter of a grain—up to the macroscopic scale—the flowing layer thickness. Therefore, no characteristic correlation length can be defined in the flowing layer. Almost 50% of flowing beads belong to these objects. We discuss recently proposed nonlocal models in the light of these experimental observations and propose an argument to explain the differences observed between granular surface flows and granular flow down a rough inclined plane.

Experimental setup.—The experimental setup is illustrated in Fig. 1a. It consists in a duralumin rotating drum of diameter $D_0 = 45$ cm and variable gap, half filled with steel beads of diameter $d = 3 \pm 0.05$ mm. Two drum thicknesses are used:

(A) A gap of 7 mm so that a quasi-2D packing is obtained but with a local 3D microscopic disordered structure. The fast camera allows us then to track the beads actually seen through the transparent sidewall of the tumbler: Around 40% of the beads are hidden and cannot be tracked.

(B) A gap of 3 mm so that a pure 2D packing is obtained and all the beads can be tracked. Additional metallic obstacles (bound to the inside of the drum) have been added in the static part of the packing to prevent any 2D ordering effects which would induce nongeneric effects. The main drawback is that the measurements can be made only during the time when the obstacles are in the bottom part of the drum.

In the recorded region, located at the center of the drum, the flowing layer thickness R and the mean angle θ of the flow can be changed by varying the rotation speed Ω. Regimes obtained for Ω varying from 1 to 8 rpm are investigated. On this range of rotating speeds, surface flows are steady and inertial effects are negligible (the Froude number $\text{Fr} = \Omega^2 D_0/2g$, g being the gravity constant, varies from 2.5×10^{-4} to 1.6×10^{-2} when Ω varies from 1 to 8 rpm).

The beads are lighted via a continuous halogen lamp. Sequences of 200 frames are recorded via a fast camera at a sampling rate of 1 kHz. The recorded region size in pixels is 480×234, one pixel corresponding to 0.227×0.227 mm. Frame processing allows us to obtain the position of the center of mass of the beads seen through the transparent side wall of the tumbler. Since the image of a single bead is made up of about 23 ± 3 pixels (depending on the distance to the sidewall), the errors on the determination of bead location is about 150 μm [12]. Tracking each bead on ten successive frames allows us to evaluate its velocity averaged on 10 ms (see Fig. 1b). The mean angle θ of the flow is calculated from the averaging of the velocity of all the beads on the whole sequence of 200 frames. The images are then divided into layers 1 bead diameter wide parallel to the flow. The mean tangential
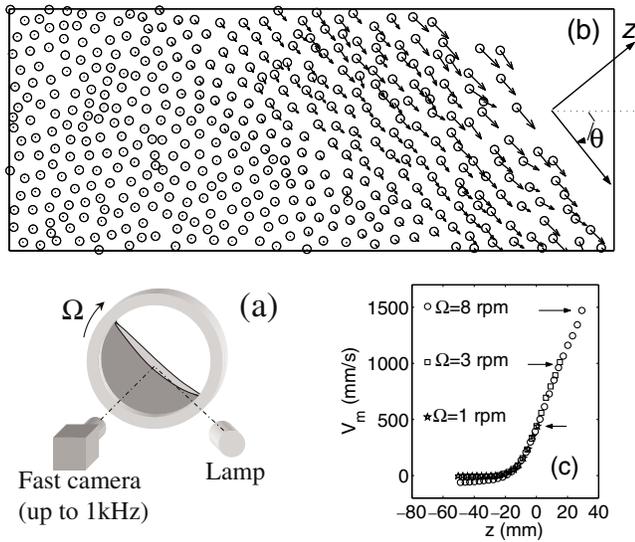
FIG. 1. (a) Sketch of the experimental setup. (b) A typical instanteous velocity field obtained for quasi-2D flows (geometry A) with $\Omega = 8$ rpm in the rectangular box of (a). (c) Velocity profile measured at the center of the drum for three different rotation speeds: $\Omega = 1$ rpm, $\Omega = 3$ rpm, and $\Omega = 8$ rpm. The arrows indicate the end of each profile. The precision on each point is better than the point size.

velocity $V_m(z)$ of the layer at depth z is then defined as the average of the velocity of all the beads of the sequence of 200 frames whose center of mass is inside the layer.

For both geometries (A) and (B), two phases can be observed: a solid phase experiencing a creep motion where V_m decreases exponentially with z (see also [13]) and a flowing phase exhibiting a clear linear velocity profile (see Fig. 1c for the quasi-2D case) with a velocity gradient $\dot{\gamma} = dV_m/dz$ independent of R, θ, the coefficient of restitution of the beads and drum gap [7]. The creep motion is not studied in this Letter. In the following, we focus on the flowing layer and neglect beads with velocities less than 100 mm/s since these are assumed to belong to the static bed.

Velocity fluctuations in quasi-2D and pure 2D flows.— In order to investigate possible collective effects, we study first the spatial correlations of the instantaneous velocity field for both geometry (A) and (B). Calling $\mathbf{V}(x, z, t)$ the velocity of a bead of the frame t located at the (x, z) coordinate in $(\mathbf{e}_x, \mathbf{e}_z)$, where the unit vector $\mathbf{e}_x$ (respectively, $\mathbf{e}_z$) is parallel (respectively, perpendicular) to the mean flow, the bead fluctuation velocity is defined as $\tilde{\mathbf{V}}(x, z, t) = \mathbf{V}(x, z, t) - V_m(z)\mathbf{e}_x$. Since the orientation of the fluctuation $\tilde{\mathbf{n}} = \tilde{\mathbf{V}}/\tilde{V}$ is not correlated to the depth z (whereas the amplitude $\tilde{V}$ of the fluctuation decreases with the depth z), we focused on the instantaneous field made up of these orientations.

One of these instantaneous fields is represented in Fig. 2a and reveals aggregates of strongly correlated beads. These correlations can be quantified by looking at the orientation-orientation correlation functions: Given
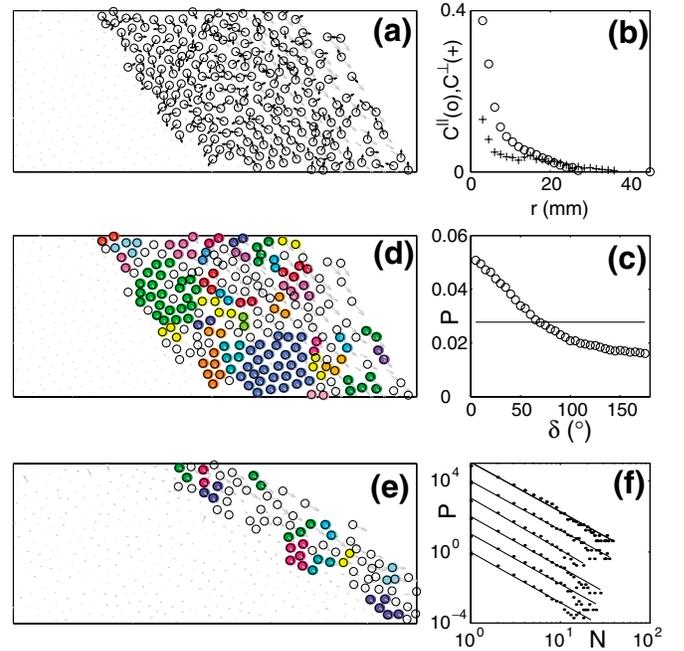

FIG. 2 (color). Clusters of beads with correlated velocity fluctuation orientation in quasi-2D flows [geometry (A)]. (a) Typical instantaneous field of the orientation of the beads velocity fluctuations obtained for a quasi-2D flow [geometry (A)] with $\Omega = 8$ rpm. The original instantaneous velocity field is represented in gray. (b) The corresponding orientation correlation functions as a function of particle separation (see text for details). (c) Distribution function $P(\delta)$ of the angle δ between the orientation of the velocity fluctuations of two beads in contact. The straight line corresponds to a uniform function. (d),(e) Typical frames of the isolated clusters, respectively, for $\Omega = 8$ rpm and $\Omega = 1$ rpm (see text for details). The position of the beads belonging to the flowing layer are represented with a black circle. The gray arrows represent the raw velocity field. Beads belonging to the same cluster are drawn in the same color (f) Probability density function of the size (in number of beads N) of these clusters. Data have been shifted for clarity. From bottom to top, $\Omega = 1$ rpm, $\Omega = 2$ rpm, $\Omega = 3$ rpm, $\Omega = 4$ rpm, $\Omega = 6$ rpm, and $\Omega = 8$ rpm. For these different Ω, i.e., for different θ and R, the distribution decreases as a power law (straight line) with the same exponent $\alpha^{(A)} = 2.9 \pm 0.1$.

two particles, labeled by 1 and 2, let $\mathbf{k}$ be the unit vector pointing from the center of 1 to the center of 2. The vector $\tilde{\mathbf{n}}_1$ has component $\tilde{n}_1^{\|}$ parallel to and $\tilde{n}_1^{\perp}$ perpendicular to $\mathbf{k}$; it is likewise for particle 2. Following [14], we define two correlation functions $C^{\|}(r) = \sum \tilde{n}_1^{\|}\tilde{n}_2^{\|}$ and $C^{\perp}(r) = \sum \tilde{n}_1^{\perp}\tilde{n}_2^{\perp}$ where the sums are over all particles such that the distance between the two particles is within $d/4$ of r. These two correlation functions reveal strong long range correlations (of the order of 30%) that extend on a range of the same order as the flowing layer thickness R (see Fig. 2b). To isolate the correlated aggregates, we have used the following criteria: Two beads i and j belong to the same cluster whenever (i) they are in contact [15] and (ii) the angle δ_{ij} between $\tilde{\mathbf{n}}_i$ and $\tilde{\mathbf{n}}_j$ is smaller than a given value δ_c arbitrarily chosen equal to 60°. This

value corresponds to the point where the experimental orientation distribution crosses the value of the uniform distribution (see Fig. 2c). Values ranging from 30° up to 90° have also been tried and do not modify the following conclusions. Figures 2d and 2e show typical frames of the individual clusters for geometry (A), respectively, for $\Omega = 8$ rpm and $\Omega = 1$ rpm. Note that the size of the largest ones is comparable to the flowing layer thickness R: The distribution of the number of beads N in a cluster is a power-law $N^{-\alpha}$ in both geometries (A) and (B), with an exponent equal, respectively, to $\alpha^{(A)} = 2.9 \pm 0.1$ and $\alpha^{(B)} = 2.0 \pm 0.1$ for quasi-2D and 2D flows (see Fig. 2f for the quasi-2D case). In both cases, the exponent is independent of Ω, i.e., independent of both R and θ. This indicates that no typical correlation length scale can be defined to characterize the spatial correlations of the velocity field.

Volume fraction fluctuations in pure 2D flows.— In order to find out the physical origin of these correlated clusters, measurements on the local volume fraction fluctuations were performed on the 2D stacking [geometry (B)]. A Voronoi tesselation can then be used to define the local volume fraction ν associated with each bead. Let us note that this technique assumes that all beads' positions are known and consequently cannot be applied for the quasi-2D packing of geometry (A). The relative fluctuations of ν are very small, a few percent (see Fig. 3a), but sufficient to alter significantly the beads' behavior. According to the "Reynolds" dilatancy concept [16], an assembly of rigid particles cannot deform whenever its volume fraction is higher than a given threshold ν_c. For pure 2D packing of monodisperse beads, $\nu_c = \pi/4$. Clusters of beads in contact with $\nu \geq \nu_c$ have been isolated in the flowing layer (see Figs. 3d–3f). Almost 50% of beads of the flowing layer belong to one of these solid clusters. As was found for the clusters defined using velocity correlation, the size of largest ones is of the order of R. The size distribution is again a power law with an exponent $\alpha_\nu^{(B)} \simeq 1.5$, weakly dependent of Ω (see Fig. 3c). This exponent is slightly smaller than the one obtained from the analysis of velocity fluctuations. It should be noted that although there is some overlap between both types of clusters, they are not identical. We have also plotted the number of beads N in a cluster against the cluster radius of gyration R_g (Fig. 3b). The power-law scaling is indicative of a fractal structure with an apparent fractal dimension equal to $d_\nu^{(B)} = 1.7 \pm 0.1$. The mean aspect ratio of the clusters, calculated as the ratio of the two principal axes of their inertia tensor, does not depend on their size and is found to be close to 2. They preferentially orient along the flow direction. Their lifetime, defined as the duration during which their size is larger than the half of their maximal size, is of order of $\sqrt{d/g} \simeq 10^{-2}$ s, where g is the gravity.

Discussion.— These solid clusters can be compared to the collective objects postulated in different nonlocal models for granular flows. Mills *et al.* [8] postulate the exis-
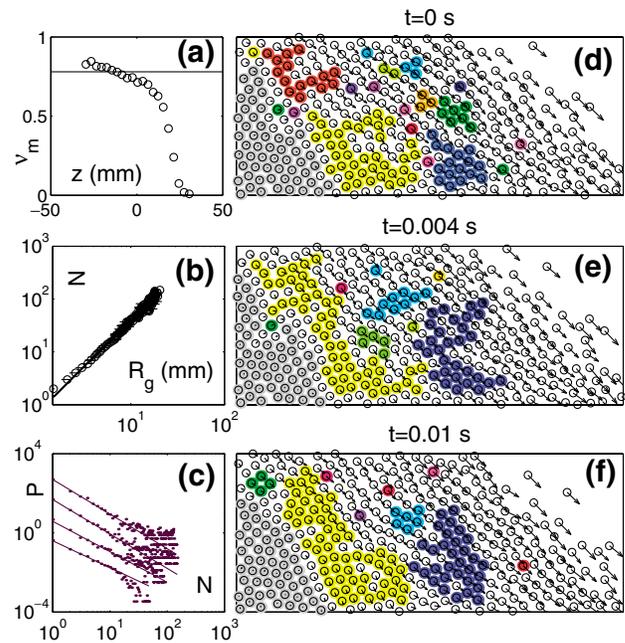

FIG. 3 (color). Presence of rigid clusters in the flowing layer of pure 2D flows [geometry (B)]. (a) Averaged volume fraction profile $\nu_m(z)$. The straight line corresponds to $\nu = \nu_c$. (b) Cluster size N plotted against their radius of gyration R_g. The error bar indicates the standard deviation on R_g of clusters with a given N. A power-law behavior (straight line) indicates fractal structures of dimension $d_f^{(A)} = 1.6 \pm 0.1$. (c) Probability density function of the size (in number of beads N) of the "rigid" clusters (see text for details). Data have been shifted for clarity. From bottom to top, $\Omega = 2$ rpm, $\Omega = 7$ rpm, $\Omega = 10$ rpm, and $\Omega = 13$ rpm. They are power law distributed with an exponent close to $\alpha_\nu^{(B)} \simeq 1.5$ weakly dependent of Ω. Frames (d), (e), and (f) show a typical sequence of these clusters. Beads belonging to the static phase appear in gray. Beads belonging to the same cluster are drawn in the same color. The clusters are tracked on the successive frames. Clusters keep their color when they remain in successive frames.

tence of 1D transient solid chains in the flowing layer, well separated from each other. In their approach, which describes granular flow down a rough inclined plane, a grain colliding with one of these chains transmits its momentum throughout the whole chain. On the other hand, for surface flows, Rajchenbach [6] suggests that each shock impact is imparted to the whole substrate beneath and thus that the momentum is "dissipated" into the whole packing. This description has been recently extended by Andreotti and Douady [10] who account for the possible trapping of flowing grains in the bumps of the static bed. The localization of the flow within a layer of finite thickness and the linear velocity profile are well reproduced in their approach. However, their model does not account for the invariance of the velocity gradient when the thickness R or the local angle θ are changed. The collective objects that we observe are neither chainlike nor the whole packing, but rather widely distributed fractal clusters involving 50% of the beads of the flowing layer. No typical length

scale can be defined. This last point may be responsible for the selection of a velocity gradient independent of both R and θ, i.e., independent of the shear stress.

The observation of the successive clusterized frames shows that the largest clusters are emitted by the static phase and die either by fragmenting into smaller ones or by sticking back to the static phase. Differences between granular flows down a rough inclined plane and granular surface flows can then be rationalized as follows: clustering results from the competition between inelastic multiple collisions, which tends to aggregate grains together [11], and shear, which erodes clusters. For flows down an inclined plane, these two effects lead to clusters of a typical size, whereas in surface flows, the static bed plays the role of a cluster reservoir: its erosion by the flowing grains can generate very large size clusters that then split and cascade into smaller and smaller ones (this mechanism might explain why we observe power-law distributions). In this view, the cluster size distribution, and *a fortiori* the velocity gradient, depend crucially on the boundary conditions.

The absence of a characteristic correlation length to describe the locally "jammed" clusters of beads is quite interesting. First, this contrasts with an assumption made in most local and nonlocal models [4,6,8,10], where the transition between the "solid" phase and the "liquid" phase is supposed to occur over a well defined length scale. The existence of multiscale rigid clusters indicates that the flowing phase is actually *critical* and suggests the proximity of a continuous "jamming" transition, of the type proposed in [17] (see also [18] for a related discussion). In this respect, it is interesting to note that similar power-law distributed clusters of strongly correlated motion have recently been observed in a colloid close to the glass transition [19].

---

[1] S. B. Savage and K. Hutter, J. Fluid Mech. **199**, 177 (1989).

[2] S. Douady, B. Andreotti, and A. Daerr, Eur. Phys. J. B **11**, 131 (1999).

[3] J. P. Bouchaud, M. E. Cates, J. R. Prakash, and S. E. Edward, J. Phys. I (France) **4**, 1383 (1994).

[4] I. S. Aranson and L. S. Tsimring, Phys. Rev. E **64**, 020301 (2001); cond-mat/0109358.

[5] M. Nagakawa, S. A. Altobeli, A. Caprihan, E. Fukushima, and E. K. Jeong, Exp. Fluids **16**, 54 (1993).

[6] J. Rajchenbach, Adv. Phys. **49**, 229 (2000).

[7] D. Bonamy, F. Daviaud, and L. Laurent, Phys. Fluids **14**, 1666 (2002); D. Bonamy, Ph.D. thesis, Université Paris XI, 2001.

[8] P. Mills, D. Loggia, and M. Tixier, Europhys. Lett. **45**, 733 (1999).

[9] T. G. Drake, J. Geophys. Res. **95**, 8681 (1990); E. Azanza, Ph.D. thesis, Ecole National des Ponts et Chaussées, 1997; O. Pouliquen, Phys. Fluids **11**, 542 (1999).

[10] B. Andreotti and S. Douady, Phys. Rev. E **63**, 031305 (2001).

[11] I. Goldhirsch, in *Physics of Dry Granular Media,* edited by H. Herrmann, J-P. Hovi, and S. Luding (Kluwer Academic Publishers, Dordrecht, 1998), p. 371; E. Falcon *et al.,* Phys. Rev. Lett. **83**, 440 (1999).

[12] For a pure 2D packing made up of weakly polydisperse, rigid smooth beads, the coordination of each bead of the bulk is four [see, e.g., C. F. Moukarzel, Phys. Rev. Lett. **81**, 1634 (1998); J.-N. Roux, Phys. Rev. E **61**, 6802 (2000)]. We thus have plotted for a static packing the distribution of the experimental contact length, i.e., of the distance between a bead and its four nearest neighbors. This distribution is Gaussian, of mean value 3 mm, and of standard deviation 50 μm. The precision on the contact length, and consequently on bead location, is thus of 150 μm with a probability of 99%.

[13] T. S. Komatsu, S. Inagaki, N. Nakagawa, and S. Nasuno, Phys. Rev. Lett. **86**, 1757 (2001).

[14] C. Bizon, M. D. Shattuck, J. B. Swift, and H. L. Swinney, Phys. Rev. E **60**, 4340 (1999).

[15] For pure 2D flows, the definition of a criterion for bead contact does not pose difficulties: two beads are in contact as soon as the distance separating their center of mass is smaller than $1.1d$. The factor 1.1 accounts for the precision in the experimental location of the beads. For quasi-2D flows, it is more complicated since the distances between beads and the sidewall of the tumbler are unknown: However, investigations on the distribution of the experimentally measured distances between a bead and its closest neighbors convince us that most beads actually seen by the camera are in contact with the tumbler sidewall. We thus have kept the same threshold for quasi-2D flows.

[16] O. Reynolds, Philos. Mag. Ser. 5 **20**, 469 (1885).

[17] A. J. Liu and S. R. Nagel, Nature (London) **396**, 21 (1998).

[18] G. D'Anna and G. Gremaud, Nature (London) **413**, 409 (2001); L. E. Silbert, D. Ertas, G. S. Grest, T. C. Halsey, and D. Levine, cond-mat/0109124.

[19] E. R. Weeks, J. C. Crocker, A. C. Levitt, A. Schofield, and D. A. Weitz, Science **287**, 627 (2000).